



Fermi National Accelerator Laboratory

FERMILAB-Pub-91/15-E
[E-581/E-704]

**Comparison of Spin Asymmetries and Cross Sections
in π^0 Production by
200-GeV Polarized Antiprotons and Protons ***

The E-581/E-704 Collaboration
Fermi National Accelerator Laboratory
P.O. Box 500
Batavia, Illinois 60510

January 7, 1991

*Submitted to *Phys. Lett.*



Operated by Universities Research Association Inc. under contract with the United States Department of Energy

Comparison of Spin Asymmetries and Cross Sections in π^0 Production by 200-GeV Polarized Antiprotons and Protons*

D.L.Adams¹⁸, N.Akchurin⁶, N.I.Belikov⁵, J.Bystricky², M.D.Corcoran¹⁸,
J.D.Cossairt³, J.Cranshaw¹⁸, A.A.Derevschikov⁵, H.En'yo⁸, H.Funahashi⁸,
Y.Goto⁸, O.A.Grachov⁵, D.P.Grosnick¹, D.A.Hill¹, K.Imai⁸, Y.Itow⁸,
K.Iwatani⁴, K.W.Krueger¹⁴, K.Kuroda¹¹, M.Laghai¹, F.Lehar²,
A.de Lesquen², D.Lopiano¹, F.C.Luehring^{15(a)}, T.Maki⁷, S.Makino⁸,
A.Masaïke⁸, Yu.A.Matulenko⁵, A.P.Meschanin⁵, A.Michalowicz¹¹,
D.H.Miller¹⁵, K.Miyake⁸, T.Nagamine^{8(b)}, F.Nessi-Tedaldi^{18(c)}, M.Nessi^{18(c)},
C.Nguyen¹⁸, S.B.Nurushev⁵, Y.Ohashi¹, Y.Onel⁶, D.I.Patalakha⁵,
G.Pauletta²⁰, A.Penzo¹⁹, A.L.Read³, J.B.Roberts¹⁸, L.van Rossum^{1,3},
V.L.Rykov⁵, N.Saito⁸, G.Salvato¹³, P.Schiavon¹⁹, J.Skeens¹⁸,
V.L.Solovyanov⁵, H.Spinka¹, R.Takashima⁹, F.Takeuchi¹⁰, N.Tamura¹⁶,
N.Tanaka¹², D.G.Underwood¹, A.N.Vasiliev⁵, A.Villari¹³, J.L.White¹⁸,
S.Yamashita⁸, A.Yokosawa¹, T.Yoshida¹⁷, A.Zanetti¹⁹.

(The FNAL E581/704 Collaboration)

- ¹ Argonne National Laboratory, Argonne, Illinois 60439, USA;
 - ² CEN-Saclay, F-91191 Gif-sur-Yvette, France;
 - ³ Fermi National Accelerator Laboratory, Batavia, Illinois 60510, USA;
 - ⁴ Hiroshima University, Higashi-Hiroshima 724, Japan;
 - ⁵ Institute of High Energy Physics, Serpukhov, USSR;
 - ⁶ Department of Physics, University of Iowa, Iowa City, Iowa 52242, USA;
 - ⁷ University of Occupational and Environmental Health, Kita-Kyushu 807, Japan;
 - ⁸ Department of Physics, Kyoto University, Kyoto 606, Japan;
 - ⁹ Kyoto University of Education, Kyoto 612, Japan;
 - ¹⁰ Kyoto-Sangyo University, Kyoto 612, Japan;
 - ¹¹ Laboratoire de Physique des Particules, BP 909, F-74017 Annecy-le-Vieux, France;
 - ¹² Los Alamos National Laboratory, Los Alamos, New Mexico 87545, USA;
 - ¹³ Dipartimento di Fisica, University of Messina, I-98100, Messina, Italy;
 - ¹⁴ Northeastern State University, Talequah, Oklahoma 74464, USA;
 - ¹⁵ Physics Department, Northwestern University, Evanston, Illinois 60201, USA;
 - ¹⁶ Okayama University, Okayama 700, Japan;
 - ¹⁷ Osaka City University, Osaka 558, Japan;
 - ¹⁸ T.W.Bonner Nuclear Laboratory, Rice University, Houston, Texas 77251, USA;
 - ¹⁹ Dipartimento di Fisica, University of Trieste, I-34100, Trieste, Italy;
 - ²⁰ University of Udine, I-33100 Udine, UD, Italy.
- (a) Present address: Indiana University, Bloomington, IN 47405, USA.
 (b) Stanford Linear Accelerator Center, Stanford, CA 94305, USA.
 (c) CERN, CH-1211 Geneva 23, Switzerland.

Abstract

The single-spin asymmetry $A_N(\bar{P}P)$ for inclusive π^0 production at $0.5 < p_t < 2$ GeV/c by 200-GeV transversely-polarized antiprotons on protons has been measured at Fermilab over a wide range of x_F . We observe that $A_N(\bar{P}P)$ has the same sign, a similar x_F dependence, and about half the magnitude as $A_N(PP)$ for π^0 production by protons. We also present the ratio of the spin-averaged cross sections for π^0 production by antiprotons and by protons.

We report the results of an experiment to measure the single-spin asymmetry $A_N(\bar{P}P)$ with transversely-polarized antiprotons for the inclusive reaction,



at $0 < x_F < 0.8$ and transverse momenta p_t ranging from 0.5 to 2 GeV/c. The parameter A_N is defined as the left-right asymmetry of the production cross section by vertically-polarized incident particles. Positive values of A_N correspond to larger cross sections for production to the beam left when the beam particle spin is vertically upward. The results are compared to $A_N(PP)$ in π^0 production by protons measured with the same apparatus and presented in Ref.[1]. These data are also used to determine the ratio of the spin-averaged cross sections for production by protons and by antiprotons as a function of x_F and p_t .

The experiment was performed using the 200-GeV antiproton beam described in Ref.[2]. The polarization of the antiprotons, arising from the decay of antilambdas, is determined by tagging the antiproton trajectories. The tagged beam polarization values, which range from $P_B = -0.65$ to 0.65 , are divided into three parts with average polarizations, $P_B = -0.45$, 0.45 , and 0 . A set of spin-rotating magnets changes the beam polarization from the transverse-horizontal to the vertical direction at the experimental target and reverses the sign of the beam polarization 5

times per hour. For a given polarity of these magnets, the same initial spin direction for antiprotons and protons is rotated into opposite vertical directions because the particle magnetic moment and spin directions are parallel for protons and antiparallel for antiprotons. The beam contains a background of about five negative pions per antiproton. A beam particle lighter than an antiproton is identified by two threshold gas Cherenkov counters.

Two photon calorimeters (detectors D1 and D2) of different design and at different distances from the target, as shown in Fig.1, were used for separate measurements of the parameter A_N . The calorimeters provide position and energy information from showers due to the photons from π^0 s produced by interactions of polarized beam antiprotons with protons in a 100-cm liquid hydrogen target.

The detector D1, located 10 m from the target, consists of 504 lead-glass counters [3] in an array of 21 columns by 24 rows offset to the left side of the beam with the first column centered on the beam axis. The size of each lead-glass block is 3.81 cm x 3.81 cm x 18 radiation lengths. The trigger rate was typically 1500 to 2000 events per 20-sec beam spill, at an average polarized antiproton intensity of 5×10^5 particles per spill. A total of 4×10^6 events was recorded with D1. The method of analysis, the efficiencies for shower identification and π^0 reconstruction in different kinematical regions, the two-photon invariant-mass resolution, and the background under the π^0 peak from uncorrelated photon pairs and π^0 s produced outside the target volume were the same as in Ref.[1] for incident protons. The two-photon invariant mass distributions for the present measurement are shown in Fig.2. The analysis uses 4.4×10^5 π^0 events from D1.

The layout, trigger conditions, and method of analysis for D2 were the same as described in Refs.[2],[4]. The detector, located at 50 m from the target and behind a sweeping magnet, consists of an array of 123 lead-glass blocks, each 6.35 cm x 6.35 cm x 13 radiation lengths. The lead-glass array is followed by a 16-layer lead-scintillator sandwich calorimeter, with 6.35 mm of lead and 1.27 cm of scintillator per layer. A scintillation counter is used to veto charged particles incident on the calorimeter. The D2 trigger required at least 30 GeV of energy to be deposited by a neutral particle, produced by interactions of polarized

antiprotons with the target. The reconstructed π^0 mass resolution was measured to be ± 17 MeV/c². The rate of background events in the mass distribution was found to be independent of the beam polarization. The number of π^0 events from D2 used in the present analysis is 4.6×10^4 .

The values of A_N measured with D1 in different regions of x_F and p_t are presented in Table I, and the combined results from D1 and D2 for A_N as a function of x_F integrated over the entire p_t region are given in Table II and Fig.3. In the intervals of x_F where both data sets cover the same p_t regions, the results from the two detectors agree within the statistical errors. The values for A_N , integrated over the p_t regions, are small and consistent with zero at $x_F < 0.2$. At larger x_F , A_N rises with increasing x_F . The p_t dependence is small at low x_F , whereas at large x_F the asymmetry as a function of p_t increases rapidly from 0 at $p_t = 0$ to $A_N \approx 0.07$ at $p_t > 0.5$.

The tables and figures show only the statistical errors. The systematic errors are small, due to the periodic reversal of the beam polarization by the spin-rotating magnets. The "beam-spin-reversal asymmetry", for events tagged with average beam polarization of zero, provides upper limits on possible false asymmetries of $\Delta A_N = 0.01$ at $x_F < 0.5$ and $\Delta A_N = 0.03$ at the largest x_F values for either detector. Systematic errors proportional to A_N such as uncertainties in the beam polarization and in subtracting the background contained in the two-photon invariant-mass distributions, are estimated to be 10 %.

Table II and Fig.3 also show A_N as a function of x_F for incident protons with data taken from Ref.[1]. The π^0 productions by protons and antiprotons are related by charge conjugation of the beam and the produced particle. The measured asymmetries have the same sign and similar x_F dependence. At large x_F , we see an indication that the magnitude of A_N for π^0 production by incident antiprotons is less than for incident protons. This implies that the interactions involve constituents in the target proton that are not invariant under charge conjugation..

The increase of A_N for $x_F \Rightarrow 1$ in both reactions suggests either a spin-dependent mechanism that dominates in the production of π^0 s at large x_F , or a production process with a spin dependence that is stronger at large x_F . The first is assumed in the fragmentation-

recombination model [5] applied to pion production with polarized beams [6]. This model attributes the asymmetry to a specific spin effect in the transfer of polarized, leading valence quarks from the beam particle to the meson produced at large x_F and small p_t . The second assumption is made in Ref.[7], which relates the observed x_F dependence of A_N to the x_F dependence of a transverse-momentum asymmetry for the constituents in transversely-polarized protons. No information exists on the energy dependence of A_N in reaction (1) since this is the first experiment using a polarized antiproton beam.

In addition to the spin asymmetries presented above, the ratio $R(\bar{P}/P)$ of the spin-averaged invariant cross sections for inclusive π^0 production by antiprotons and protons has been determined from the measurement presented here and the corresponding measurement [1] with incident protons. The beam line is readily changed from antiprotons to protons without any change of the geometry for the beam, target, and detector. Therefore, the acceptance of the detectors, and the efficiencies for shower identification and π^0 reconstruction in different kinematical regions, cancel in the determination of R .

The results for R as a function of x_F and p_t , measured with D1, are presented in Table III and Figure 4, and show a strong dependence on kinematics. The statistical accuracy is substantially better than in previous measurements [8] of R with unpolarized beams containing fewer antiprotons. The difference in π^0 production by antiprotons and by protons is largest for high-energy π^0 s produced at small angles with the beam. At large x_F and small p_t , the ratio R is close to $R = 2$ and decreases rapidly with increasing transverse momentum, while at $x_F < 0.3$, one observes ratios between $R = 1.0$ and 1.3 at all values of p_t .

The ratio of the spin asymmetries is $A_N(\bar{P}P)/A_N(PP) = 0.54 \pm 0.18$, and the ratio of the spin-averaged cross sections is $R = 1.50 \pm 0.01$, averaged over the kinematical region $0.5 < x_F < 0.8$ and $0.6 < p_t < 2$ GeV/c. In this region, unpolarized antiprotons produce 1.5 times more π^0 s and the relative difference between the cross sections for opposite antiproton-spin states is about one-half that for opposite proton-spin states.

The first high-energy data for (a) the asymmetry A_N in the reaction $\bar{P} + P \Rightarrow \pi^0 + X$, (b) the asymmetry A_N in the reaction $P + P \Rightarrow$

$\pi^0 + X$, and (c) the ratio $R(\bar{P}/P)$ of the spin-averaged production cross sections provide a large amount of input and significant constraints for the phenomenology of "soft" pion production by protons and antiprotons in definite transverse-spin states. The interpretation of the results involves assumptions about the internal spin structure of transversely-polarized protons and antiprotons, leading to different explanations how the beam-polarization information is transmitted in the π^0 production process.

We would like to acknowledge useful discussions of theoretical issues with colleagues at our respective institutions. We gratefully acknowledge the assistance of the staff of Fermilab and of all the participating institutions. This research was supported by the U.S.S.R. Ministry of Atomic Power and Industry, the Ministry of Education, Science, and Culture in Japan, the U.S. Department of Energy, the Commissariat a l'Energie Atomique and the Institut National de Physique Nucleaire et de Physique des Particules in France, and the Istituto di Fisica Nucleare in Italy.

* This work was performed at the Fermi National Accelerator Laboratory, which is operated by University Research Associates, Inc., under contract DE-AC02-76CH03000 with the U.S. Department of Energy.

Work supported in part by the U.S. Department of Energy, Division of High Energy Physics, Contracts W-31-109-ENG-38, W-7405-ENG-36, DE-AC02-76ER02289, DE-AS05-76ER05096.

REFERENCES

- [1] D.L.Adams et al., Preprint FERMILAB-Pub-91/13-E,Jan.7,1991,
submitted to Phys.Rev.Lett.
- [2] D.P.Grosnick et al., Nucl.Instr.Meth.A290(1990)269.
- [3] N.I.Belikov et al., to be submitted to Nucl.Instr.Meth.
- [4] Bonner et al., Phys.Rev.Lett.61(1988)1918.
- [5] T.DeGrand and H.I.Miettinen,
Phys.Rev.D24(1981)2419.
- [6] N.M.Krishna, Ph.D.Thesis,Rice University,Oct.1989.
M.G.Ryskin, Sov.J.Nucl.Phys.48(4)(1989)708.
- [7] D.Sivers, Phys.Rev.D41(1990)83.
- [8] G.Donaldson et al., Phys.Rev.Lett.40(1978)917.

FIGURE CAPTIONS

- Fig. 1 The schematic layout of the apparatus.
- Fig. 2 The two-photon invariant-mass distributions for detector D1 for (a) $0 < x_F < 0.1$, (b) $0.4 < x_F < 0.5$, and (c) $0.5 < x_F < 0.8$.
- Fig. 3 The asymmetries A_N in the reactions $\bar{P} + P \Rightarrow \pi^0 + X$ (closed circles) and $P + P \Rightarrow \pi^0 + X$ (open squares, see Ref.[1]) at 200 GeV in different regions of x_F , integrated over p_t from 0.5 to 2 GeV/c. $\sigma^{\uparrow}/\sigma^{\downarrow}$ is the ratio of the π^0 production cross sections for opposite beam spins.
- Fig. 4 The ratio $R(\bar{P}/P)$ of the spin-averaged cross section for π^0 production by antiprotons and by protons. The dotted lines are added to guide the eye.

TABLE I. The asymmetry parameter A_N for inclusive π^0 production by 200-GeV antiprotons given as a function of both p_T and x_F .

x_F	p_T (GeV/c)	A_N (%)
0.0-0.3	0.5-0.7	1.7 ± 1.1
	0.7-0.9	0.0 ± 1.7
	0.9-1.3	2.8 ± 2.1
	1.3-2.0	3.2 ± 4.3
0.3-0.4	0.5-0.7	1.2 ± 2.1
	0.7-0.9	1.8 ± 2.9
	0.9-1.3	-2.5 ± 3.4
	1.3-2.0	2.5 ± 6.7
0.4-0.5	0.5-0.7	3.1 ± 2.5
	0.7-0.9	3.6 ± 3.4
	0.9-1.3	10.0 ± 4.0
	1.3-2.0	14.5 ± 8.9
0.5-0.8	0.5-0.7	7.0 ± 2.8
	0.7-0.9	7.5 ± 3.7
	0.9-1.3	7.1 ± 4.1
	1.3-2.0	11.5 ± 8.7

TABLE II. The asymmetry parameters A_N for inclusive π^0 production by 200-GeV polarized antiproton and proton beams, respectively, for different regions of x_F and averaged over different p_T regions. Data given in the last column is taken from Ref. 3.

x_F	$\langle x_F \rangle$	p_T	$\langle p_T \rangle$	No. π^0 Events	A_N \bar{p} beam (%)	A_N p beam (%)
		(GeV/c)	(GeV/c)			
0.0-0.1	0.03	0.5-2.0	0.7	60 300	1.6 ± 1.4	-0.1 ± 1.2
0.1-0.2	0.13	0.5-2.0	0.7	151 600	0.4 ± 0.9	0.8 ± 0.8
0.2-0.3	0.23	0.5-2.0	0.7	117 100	2.9 ± 0.9	0.7 ± 1.0
0.3-0.4	0.33	0.6-2.0	0.8	87 800	3.1 ± 1.1	4.1 ± 1.0
0.4-0.5	0.43	0.7-2.0	0.9	44 600	5.0 ± 1.6	6.2 ± 1.1
0.5-0.6	0.53	0.8-2.0	0.9	19 600	6.8 ± 2.4	11.5 ± 1.6
0.6-0.8	0.67	0.8-2.0	1.0	7 300	7.2 ± 3.7	15.0 ± 2.7

TABLE III. The ratio of the spin-averaged invariant cross sections for the reactions, $\bar{p}\uparrow + p \rightarrow \pi^0 + X$ and $p\uparrow + p \rightarrow \pi^0 + X$ at 200 GeV, given as a function of both p_T and x_F .

p_T (GeV/c)	x_F	Ratio \bar{p}/p	p_T (GeV/c)	x_F	Ratio \bar{p}/p
0.4-0.6	0.0-0.1	1.22 ± 0.01	1.2-1.4	0.0-0.1	1.10 ± 0.04
	0.1-0.2	1.25 ± 0.01		0.1-0.2	1.07 ± 0.03
	0.2-0.3	1.26 ± 0.01		0.2-0.3	1.03 ± 0.03
	0.3-0.4	1.44 ± 0.01		0.3-0.4	1.11 ± 0.03
	0.4-0.5	1.70 ± 0.02		0.4-0.5	1.16 ± 0.04
	0.5-0.6	2.00 ± 0.03		0.5-0.6	1.35 ± 0.05
	0.6-0.8	...		0.6-0.8	1.44 ± 0.08
0.6-0.8	0.0-0.1	1.19 ± 0.01	1.4-1.6	0.0-0.1	1.09 ± 0.06
	0.1-0.2	1.21 ± 0.01		0.1-0.2	1.07 ± 0.04
	0.2-0.3	1.23 ± 0.01		0.2-0.3	1.05 ± 0.04
	0.3-0.4	1.25 ± 0.01		0.3-0.4	1.01 ± 0.04
	0.4-0.5	1.31 ± 0.02		0.4-0.5	1.12 ± 0.05
	0.5-0.6	1.54 ± 0.03		0.5-0.6	1.25 ± 0.07
	0.6-0.8	...		0.6-0.8	1.30 ± 0.10
0.8-1.0	0.0-0.1	1.13 ± 0.01	1.6-2.0	0.0-0.1	1.04 ± 0.06
	0.1-0.2	1.12 ± 0.01		0.1-0.2	1.01 ± 0.04
	0.2-0.3	1.12 ± 0.01		0.2-0.3	1.04 ± 0.03
	0.3-0.4	1.19 ± 0.01		0.3-0.4	1.03 ± 0.05
	0.4-0.5	1.23 ± 0.02		0.4-0.5	1.04 ± 0.06
	0.5-0.6	1.38 ± 0.03		0.5-0.6	1.26 ± 0.08
	0.6-0.8	1.84 ± 0.05		0.6-0.8	1.28 ± 0.10
1.0-1.2	0.0-0.1	1.12 ± 0.02			
	0.1-0.2	1.09 ± 0.02			
	0.2-0.3	1.09 ± 0.02			
	0.3-0.4	1.12 ± 0.02			
	0.4-0.5	1.21 ± 0.03			
	0.5-0.6	1.30 ± 0.04			
	0.6-0.8	1.65 ± 0.07			

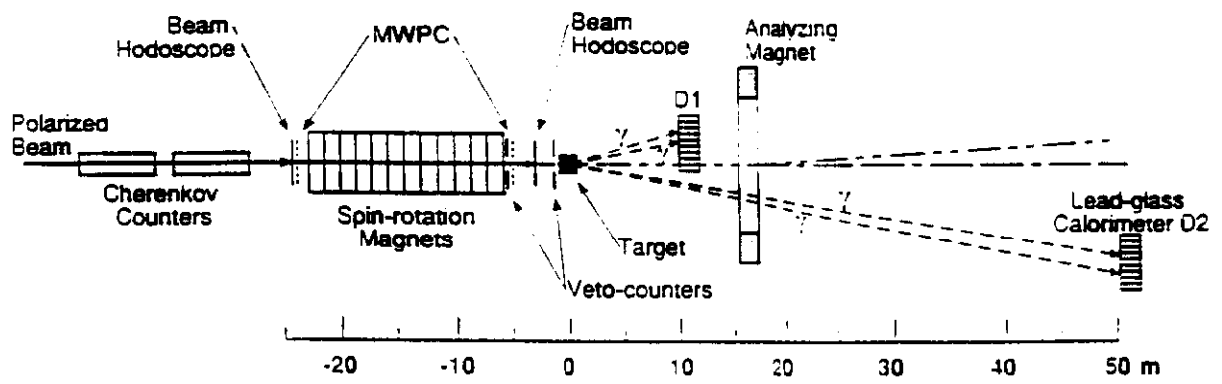


Figure 1

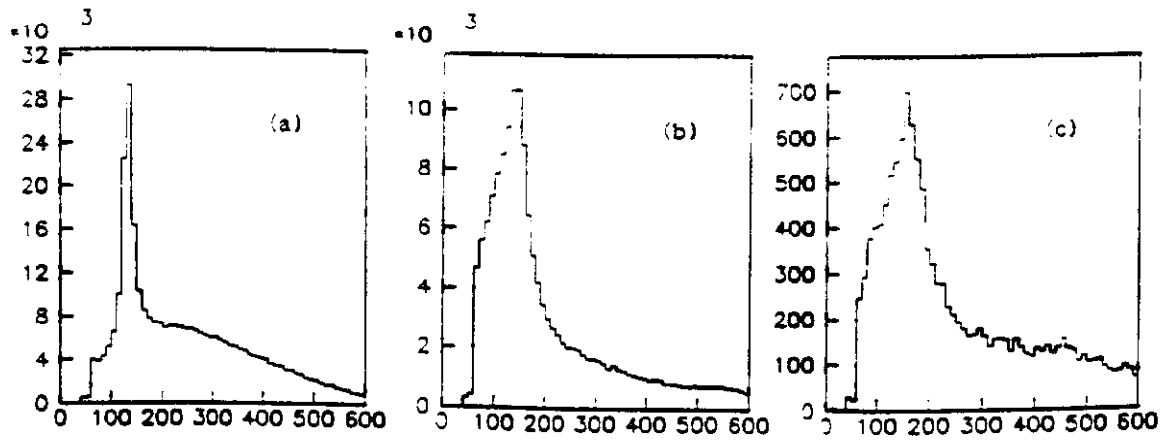


Figure 2

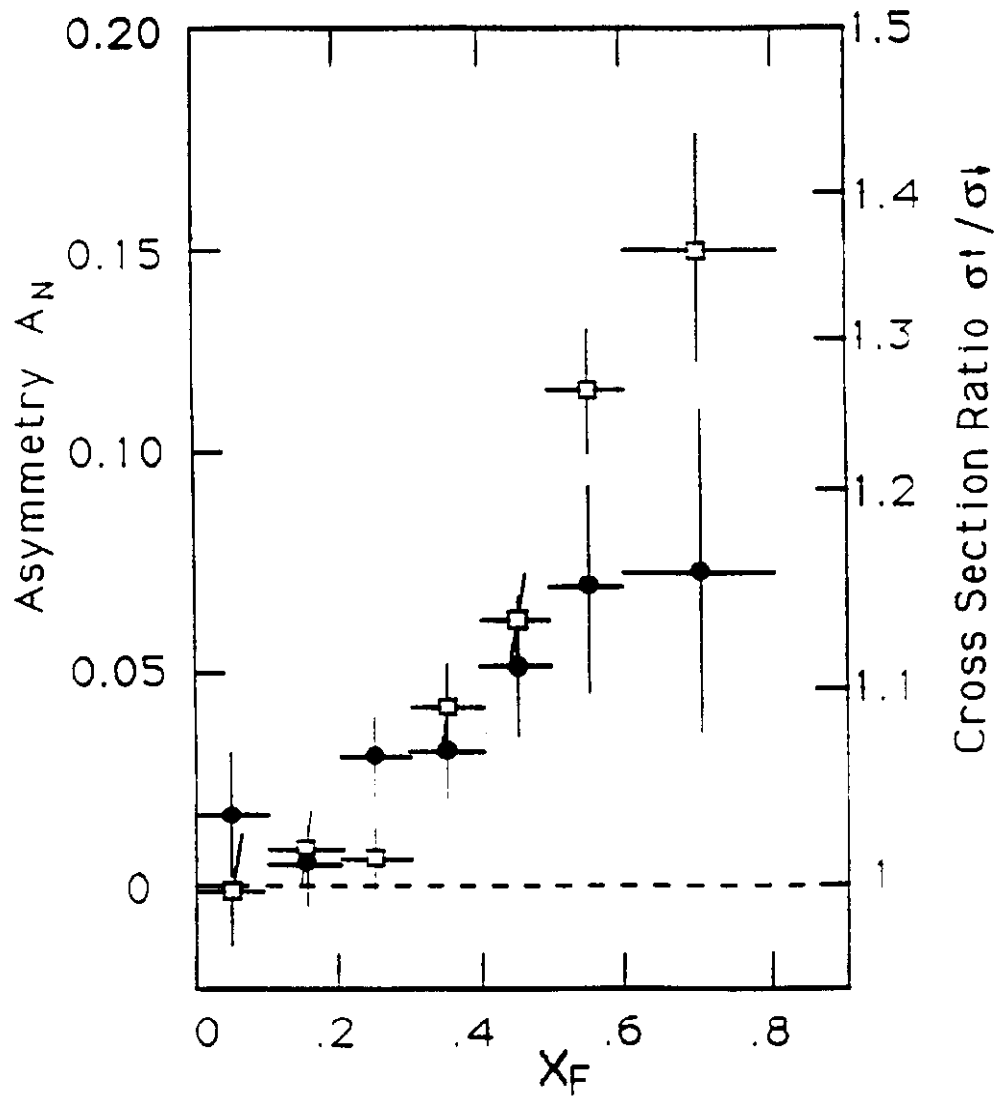


Figure 3

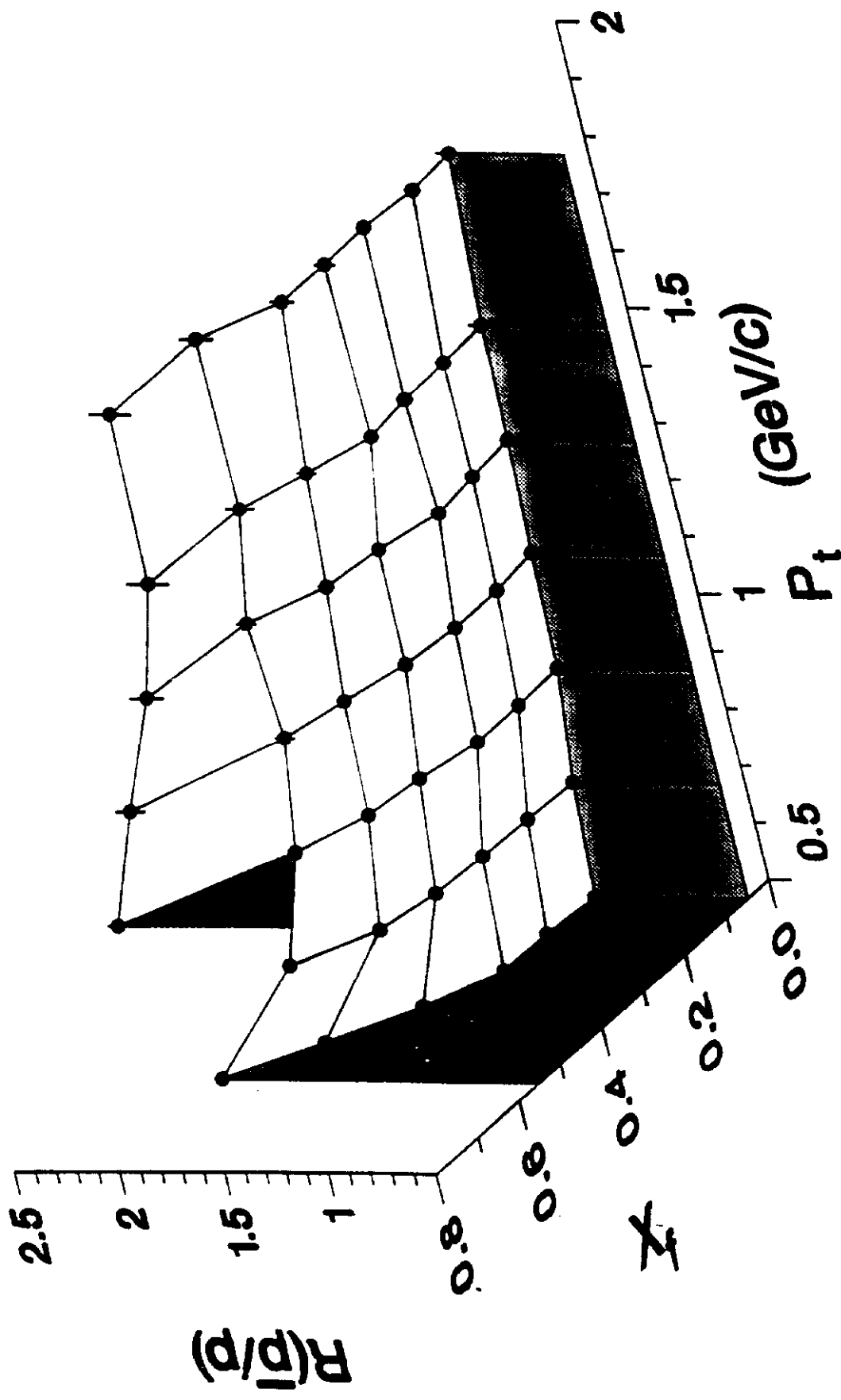


Figure 4